Improvement of track segment association with classification information

Benjamin Pannetier, Jean Dezert

Improvement of track segment association with classification information

Benjamin Pannetier, *Member, ISIF* and Jean Dezert, *Member, ISIF*

ONERA, The French Aerospace Lab, F-91761 Palaiseau, France.

E-mail: benjamin.pannetier@onera.fr, jean.dezert@onera.fr

Abstract

In this paper, we propose a full process to track ground targets and correct the ground tactical situation. The ground target tracking is done at each scan time of a Ground Moving Target Indicator (GMTI) airborne sensor. The algorithm takes into account the road network in the tracking process to improve the track precision and an Interacting Multiple Model (IMM) to deal with maneuvers of the targets. The multiple target tracking algorithm based on Structured-Branching Multiple Hypothesis Tracker (SB-MHT) improves significantly the track precision and continuity. However, because of subversive target maneuvers (a target can deliberately stop to avoid to be detected by GMTI sensor), the airborne sensor maneuver who carries along the cut-off of the sensor, or because of a possible poor road network modelling, the obtained tracks are not always properly updated and can be automatically and erroneously deleted by classical algorithms. To circumvent this serious problem, we propose an extension of our previous work to correct the current situation with past situation in order to correlate current tracks with past tracks and solve the track segment association problem. The correlation between current tracks with old ones is based on kinematic and classification information. The performances of this global process are quantified on a simulated scenario considering twenty maneuvering ground targets observed by one airborne with a GMTI sensor and Unattended Ground Sensor (UGS).

Index Terms

Ground target tracking, track segment association, information fusion.

Manuscript submitted May xx, 2012.

CONTENTS

AEKF Alternative Extended Kalman Filter

BDTOPO Base de Données TOPOgraphiques

DSmT Dezert-Smarandache Theory

DTED Digital Terrain Elevation Data

EKF Extended Kalman Filter

GIS Geographic Information System

GMTI Ground Moving Target Indicator

HRRR High Range Radial Resolution

IMM Interacting Multiple Model

JBPDAF Joint Belief Probabilistic Data Association Filter

JPDAF Joint Probabilistic Data Association Filter

LLR Log-Likelihood Ratio

MDV Minimal Detectable Velocity

MHT Multiple Hypothesis Tracker

MOP Measure Of Performance

MTI Moving Target Indicator

MTL Mean Track Life

NATO North ATlantic Organization

PCC Percentage of Correct Classification

PHD Probability Hypotheses Density

RSS SPRT Road Set Segment based on Sequential Probability Ratio Test

RTS Rauch Tung Striebel

SB-MHT Structured-Branching Multiple Hypothesis Tracker

SNR Signal to Noise Ratio

SPRT Sequential Probability Ratio Test

STANAG STAndardization Nato AGreement

TCF Topographic Coordinate Frame

TSA Track Segment Association

TSP Track Segment Purity

UAV Unnamed Aerial Vehicle

UGS Unattended Ground Sensor

VS IMM Variable Structure Interacting Multiple Model

VS IMMC Variable Structure Interacting Multiple Model under Constraint

WGS84 World Geodetic System 1984

I. Introduction

Tracking ground targets with several sensors is crucial in order to establish the situation awareness and the threat assessment on the battlefield. Since several years, ground targets tracking algorithms have been studied and integrated in fusion stations. The principal challenge is to adapt or develop new ground tracking algorithms to ensure the track continuity and improve the intelligence functionality.

Ground tracking algorithms are used in a special environment: the high traffic density and the large number of false alarms, that brings about a significant data quantity, the strong and fast target maneuvers which compromise target tracking due to the association problem and the terrain elevation that generates undetected areas in which ground targets cannot be detected. In a Ground Moving Target Indicator (GMTI) surveillance context, we propose to use the road network information as a prior information in order to improve the tracking quality. Under the assumption that the targets are evolving on the road network and using a Bayesian approach, we introduce the event that the target state belongs to a road segment (*i.e.* the position is on the road segment and the velocity in the road segment direction). In previous work, it has been shown that an adequate constrained motion model followed by the pseudo projection of the estimated state is a good approach to constraint the state to the road [1].

In addition, the use of identification information is necessary in a context where the target

evolve in the same area. Because of the ground target proximity and the sensor precision, the kinematic discrimination is not sufficient to maintain the correct association between tracks and measurement. In [2], a general expression for multi-sensor data association that includes attribute information is presented. In [3], [4], the authors present a new tracking algorithm called Joint Belief Probabilistic Data Association Filter (JBPDAF), which uses both track fusion and target identification features. The features are obtained according the High Range Radial Resolution (HRRR) of the GMTI sensor. This approach was extended and adapted later to the EO/IR sensor in [5]. In [6], the authors propose a bayesian inference to update the classification vector of a target and they modify the cost of the assignment by using kinematic information and classification information. The adaptation of d the previous approach to the Structured-Branching Multiple Hypothesis Tracker (SB-MHT) [2] has been done in [7] with the use of Dezert-Smarandache Theory (DSmT) to update and to modify the assignment cost. The feature information was provided by an aerial EO/IR system.

Despite of the track assignment improvement due to joint use of identification and kinematic information, the use of the tracker is limited in time due to the Unnamed Aerial Vehicle (UAV) performances (maneuvers, autonomy, ...) and the classification information given by the GMTI sensor are weak. In fact, in the first case, the GMTI sensor is shut down during a long time period that implies to reboot the tracker and therefore we cannot avoid the track breakage between the past situation and the current situation. In the second case, we work with the constraint of non-using HRRR (so the track obtained with GMTI sensors have a weak classification level). In addition, the proportion of well-classified tracks obtained after the fusion between GMTI tracks and EO/IR UAV detections is very small (the number of track given by the GMTI sensor is significantly higher than the track number combined with the EO/IR detections because the sensor area coverage of this sensor is negligible with respect to the coverage of the GMTI sensor). To palliate the track breakage and the weak track classification, we propose in this paper a new approach to solve the Track Segment Association (TSA) problem presented in [8] by using classification information obtained with Unattended Ground Sensor (UGS). The advantage to use UGS is the repartition of several *in-situ* sensors on a big area surveillance that are able to provide a well-classification information about targets.

The TSA is topic of interest to correlate or to correct current tactical situation with past situation. This is the case if the sensors can't provided data in an area of interest or if we want

to use a tactical situation given by another system in a distributed network.

The part II of this paper presents a brief description of the contextual information and the modeling of the target state under constraint in the two dimensional space, and the mathematical expressions of the Moving Target Indicator (MTI) and Unattended Ground Sensor (UGS) measurements. The part III is devoted to: 1) the construction of the IMM with a variable set of constraint motion models in order to track the maneuvering targets on the road network, 2) the description of the detection of the off-road dynamic, and 3) the integration of the classification information in the Structured-Branching Multiple Hypothesis Tracker (SB-MHT) to improve the discrimination between the tracks and measurement. In the part IV, the Track Segment Association (TSA) algorithm is detailed to show how we integrate the track classification information in the score association used for the TSA. Simulation results obtained in a complex realistic Multiple Ground Targets Tracking Scenario within a real environment are presented and analyzed in Part V, before concluding this paper.

II. Motion and observation models

A. GIS description

The Geographic Information System (GIS) used in this work contains the following information: the segmented road network and Digital Terrain Elevation Data (DTED). The road network is connected and each road segment is indexed by the road section it belongs to. A road section is defined by a finite set of connected road segments delimited by a road end or a junction. For the topographic information we use the database called: BD TOPO[1]. This Geographic Information System (GIS) has a metric precision on the roads segments location. At the beginning of a surveillance battlefield operation, a Topographic Coordinate Frame (TCF) and its origin *O* are chosen in the manner that the axes *X*, *Y* and *Z* are respectively oriented in the east, north and up local direction. The target tracking process is carried out in the Topographic Coordinate Frame (TCF). In addition, starting from the DTED and the sensor location at the current time, it is possible to compute the perceivability (noted P_e) at any point of the DTED. A function named $P_e(x, y, k)$ indicates if the pixel of the DTED at the location (x, y) is observable by the sensor or not at time k.

[1]See www.ign.fr/rubrique.asp?lng_id=EN&rbr_id1621 for a description of this Geographic Information System (GIS).

B. Constrained motion model

The target state at the current time t_k is defined in the local horizontal plane of the Topographic Coordinate Frame (TCF) by the vector:

$$\mathbf{x}(k) = [x(k)\ \dot{x}(k)\ y(k)\ \dot{y}(k)]^T \tag{1}$$

where (x_k, y_k) and $(\dot{x}_k, \dot{y}_k)$ define respectively the target location and velocity in the local horizontal plane. The dynamics of the target evolving on the road are modeled by a first-order differential system. The target state on the road segment s is defined by $\mathbf{x}_k^s$ where the target position (x_k^s, y_k^s) belongs to the road segment s and the corresponding heading $(\dot{x}_k^s, \dot{y}_k^s)$ in its direction.

The event that the target is on road segment s is noted $e_k^s = \{\mathbf{x}_k \in s\}$. Given the event e_k^s and according to a motion model $\mathcal{M}_i$, the estimation of the target state can be improved by considering the road segment s. For a constant velocity motion model, it follows:

$$\mathbf{x}_k^s = \mathbf{F}^{s,i}(\Delta_k) \cdot \mathbf{x}_{k-1}^s + \mathbf{\Gamma}(\Delta_k) \cdot \mathbf{v}_k^{s,i} \tag{2}$$

where Δ_k is the sampling time, $\mathbf{F}^{s,i}$ is the state transition matrix associated to the road segment s and adapted to a motion model $\mathcal{M}_i$; $\mathbf{v}_k^{s,i}$ is a white zero-mean Gaussian random vector with covariance matrix $\mathbf{Q}_k^{s,i}$ chosen in such a way that the standard deviation σ_d along the road segment is higher than the standard deviation σ_n in the orthogonal direction. It is defined by:

$$\mathbf{Q}_k^{s,i} = \mathbf{R}_{\theta_s} \cdot \begin{pmatrix} \sigma_d^2 & 0 \\ 0 & \sigma_n^2 \end{pmatrix} \cdot \mathbf{R}_{\theta_s}^{'} \tag{3}$$

where $\mathbf{R}_{\theta_s}$ is the rotation matrix associated with the direction θ_s defined in the plane (O, X, Y) of the road segment s. The matrix $\mathbf{\Gamma}(\Delta_k)$ is defined in [9].

To improve the modeling for targets moving on a road network, we have proposed in [10] to adapt the level of the dynamic model's noise based on the length of the road segment s. The idea is to increase the standard deviation σ_n defined in (3) to take into account the error on the road segment location. After the state estimation obtained by a Kalman filter, the estimated state is then projected according to the road constraint e_k^s. This process is detailed in [11].

C. Measurement model

1) MTI report segment: According to the GMTI STAndardization Nato AGreement (STANAG) [12], the MTI reports received at the fusion station are expressed in the World Geodetic System 1984 (WGS84) coordinates system. The MTI reports must be converted in the TCF. A MTI measurement $\mathbf{z}_k^{MTI}$ at the current time t_k is given in the TCF by:

$$\mathbf{z}_k^{MTI} = [x_k \ y_k \ \dot{\rho}_k]^T \tag{4}$$

where (x_k, y_k) is the location of the MTI report in the local frame (O, X, Y) and $\dot{\rho}_k$ is the associated range radial velocity measurement expressed by:

$$\dot{\rho}_k = \frac{(x_k - x_{c,k}) \cdot \dot{x}_k + (y_k - y_{c,k}) \cdot \dot{y}_k}{\sqrt{(x_k - x_{c,k})^2 + (y_k - y_{c,k})^2}} \tag{5}$$

where $(x_{c,k}, y_{c,k})$ is the sensor location at the current time in the TCF.

Because the range radial velocity is correlated to the MTI location components, the use of an Extended Kalman Filter (EKF) is not adapted. In the literature, several techniques exist to uncorrelate the range radial velocity from the location components. We prefer to use the Alternative Extended Kalman Filter (AEKF) proposed by Bizup and Brown in [13], because the implementation is easier by using the alternative linearization than another algorithms to decorrelate the components. Moreover, AEKF remains invariant by translation when working in the sensor referential/frame. The Alternative Extended Kalman Filter (AEKF) measurement equation is given by:

$$\mathbf{z}_k^{MTI} = \mathbf{H}_k^{MTI} \cdot \mathbf{x}_k + \mathbf{w}_k^{MTI} \tag{6}$$

where $\mathbf{w}_k^{MTI}$ is a zero-mean white Gaussian noise vector with a covariance $\mathbf{R}_k^{MTI}$. The observation matrix $\mathbf{H}_k^{MTI}$ is defined by:

$$\mathbf{H}_k^{MTI} = \begin{pmatrix} 1 & 0 & 0 & 0 \\ 0 & 0 & 1 & 0 \\ 0 & \frac{\partial \dot{\rho}_k}{\partial \dot{x}} & 0 & \frac{\partial \dot{\rho}_k}{\partial \dot{y}} \end{pmatrix} \tag{7}$$

The explicit expression of (7) is given in [13]. However, due to the STANAG 4607 it is impossible to know the correlation coefficient between the location (x_k, y_k) and range radial velocity components $\dot{\rho}$. In fact, the components are dependent because the range radial velocity depends on the Doppler measurement and the location is obtained with Doppler measurement

too. Then a crude assumption is used in order to built the covariance $\mathbf{R}_k^{MTI}$ of $\mathbf{w}_k^{MTI}$: we assume here that the correlation factor is null. So the covariance is approximated by :

$$\mathbf{R}_k^{MTI} = \begin{pmatrix} \sigma_{\mathrm{x}}^2 & \sigma_{\mathrm{xy}}^2 & 0 \\ \sigma_{\mathrm{xy}}^2 & \sigma_{\mathrm{y}}^2 & 0 \\ 0 & 0 & \sigma_{\dot{\rho}}^2 \end{pmatrix} \tag{8}$$

where the left upper 4×4 submatrix represents the well-known covariance in location expressed in the TCF. $\sigma_{\dot{\rho}}^2$ is the standard deviation of the modified range radial velocity and σ_{xy}^2 is the cross-covariance. Each MTI report is characterized both with the location and velocity information and also with the attribute information and the probability that it is correct. We denote C_{MTI} the frame of discernment on target ID based on MTI data. C_{MTI} is assumed to be constant over the time and consists in a finite set of exhaustive and exclusive elements representing the possible states of the target classification. In this paper, we consider only 3 elements in C_{MTI} defined as $C_{MTI} = \{$*Tracked vehicle*, *Wheeled vehicle*, *Rotary wing aircraft*$\}$.

We consider also the probabilities $P(c_k)$ ($\forall c_k \in C_{MTI}$) as input parameters of our tracking systems characterizing the global performances of the classifier. The values c_k and $P(c_k)$ are the outputs of the classifier. The vector of probabilities $[P(c_k = 1)\ P(c_k = 2)\ P(c_k = 3)]$ represents the diagonal of the "confusion matrix" $\mathbf{C}_k = [c_k^{i,j}]$ of the classification algorithm assumed to be used. As in [6], the elements of the "confusion matrix" is the likelihood of the true class being i when the classifier output is j.The other terms of this matrix are unknown. So, the other terms are extrapolated in the manner the sum of column i is equal to one.

We denote by $\mathbf{z}_k^{MTI\star}$ the extended MTI measurements including both kinematic part and attribute part defined by

$$\mathbf{z}_k^{MTI\star} \triangleq \{\mathbf{z}_k^{MTI}, c_k, P(c_k)\} \tag{9}$$

2) UGS report segment: For the UGS intelligence systems, we consider two sensor types: a video EO/IR sensor and an acoustic sensor fixed on a Unattended Ground Sensor (UGS). We assume that the reports are expressed in the reference frame (O, X, Y) and give a location information and type information of the target. A UGS measurement z^{UGS} at the current time t_k is given in the TCF by

$$\mathbf{z}_k^{UGS} = [x(k)\ y(k)]' \tag{10}$$

The measurement equation is given by:

$$\mathbf{z}_k^{UGS} = \mathbf{H}_k^{UGS} \cdot \mathbf{x}(k) + \mathbf{w}_k^{UGS} \tag{11}$$

where $\mathbf{H}_k^{UGS}$ is the observation matrix of the video sensor given by

$$\mathbf{H}_k^{UGS} = \begin{pmatrix} 1 & 0 & 0 & 0 \\ 0 & 0 & 1 & 0 \end{pmatrix} \tag{12}$$

The white noise Gaussian process $\mathbf{w}_k^{UGS}$ is centered and has a known covariance $\mathbf{R}_k^{UGS}$ given by the ground station.

We denote $\mathbf{z}_k^{UGS\star}$ the extended video measurements including both kinematic part and attribute part defined $\forall c_k \in C_{UGS}$ by

$$\mathbf{z}_k^{UGS\star} \triangleq \{\mathbf{z}_k^{UGS}, c_k, P(c_k)\} \tag{13}$$

The attribute type of the Unattended Ground Sensor (UGS) sensors belongs to a different and better classification than the Moving Target Indicator (MTI) sensors. This classification set is based on a taxonomy presented in the following subsection.

D. Taxonomy

In our work, the symbology 2525C [14] is used to describe the links between the different classification sets C_{MTI} and C_{UGS}. Figure 1 represents a short part of the 2525C used in this paper. The red elements underlined in italic style are the atomic elements of our taxonomy and define the common classification set denoted C_{2525C}. Each element of both sets can be placed in Figure 1. For example, the "wheeled vehicle" of the set C_{MTI} is placed at the level "Armoured $\rightarrow$ Wheeled" or the "Volkswagen Touareg" given by the Unattended Ground Sensor (UGS) is placed at the levels "Armoured $\rightarrow$ Wheeled$\rightarrow$ Medium" and "Civilan Vehicle $\rightarrow$ Jeep $\rightarrow$ Medium". In general, each elements of C_{MTI} and C_{UGS} are associated to a sub-set of C_{2525C}. The associated probability at current time t_k is obtained by the following refinement process:

$$(\forall c_k \in C_{MTI})(\exists J \subset C_{2525C})(\forall a_k^j \in J) \bigcup_{j \in J} a_k^j = c_k, P_J(a_k^j) = \frac{P(c_k)}{N} \tag{14}$$

where J is the list of attributes that characterize the element c_k of C_{MTI} and $N = \mid \bigcup_{j \in J} a_k^j \mid$. The likelihood function obtained after the refinement process respects the following condition:

$$\sum_{j \in C_{2525C}} P_J(a_k^j) = 1 \tag{15}$$

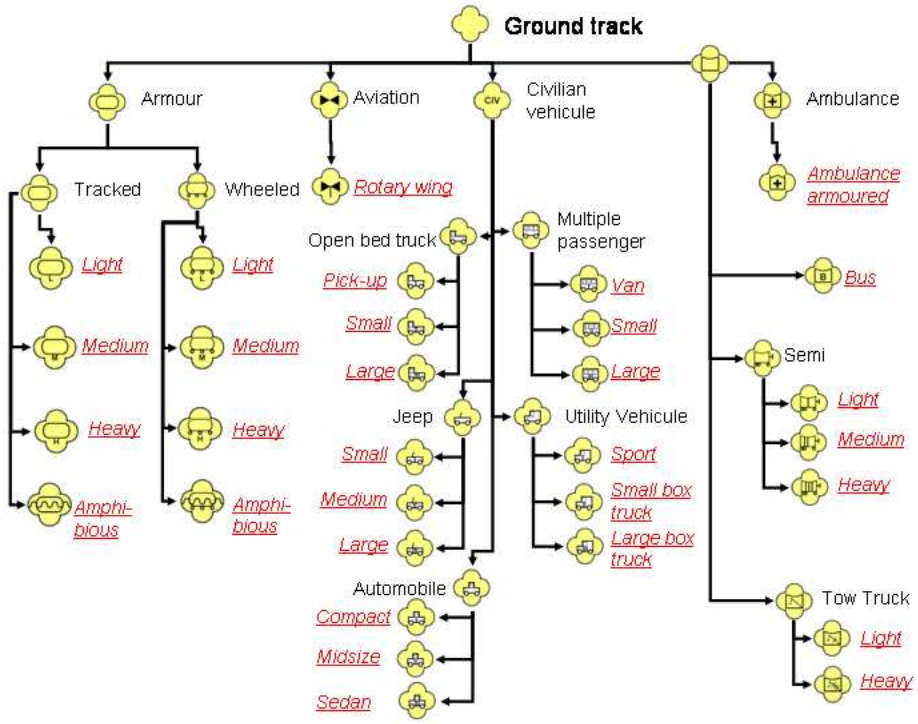

Figure 1: 2525C (light version).

The refinement process is similar for the set C_{UGS}.

For notation convenience, the measurements sequence $Z^{k,l} = \{Z^{k-1,n}, \mathbf{z}_k^j\}$ represents a possible set of measurements generated by the target up to time k. $Z^{k,l}$ consists in a subsequence $Z^{k-1,n}$ of measurements up to time $k-1$ and a validated measurement $\mathbf{z}_k^j$ available at time k associated with the track $\mathcal{T}^{k,l}$. At the current time *k*, the track $\mathcal{T}^{k,l}$ is represented by a sequence of the state estimates.

III. Variable Structure Interacting Multiple Model under Constraint

A. IMM under road segment constraint

The IMM is an algorithm for combining estimated states from multiple models to get a better state estimate when the target is maneuvering. The IMM is near optimal with a reasonable complexity. In section II-B, a constrained motion model i to segment s, noted $\mathcal{M}_k^{s,i}$, was defined. There is a distinction between the definition of a motion model $\mathcal{M}_k^{s,i}$ (*i.e.* motion model type, noise,...) and the event $M_k^{s,i}$ that the target is moving on the road according the motion model

i at time k. Here we extend the segment constraint to the different dynamic models (among a set of $r+1$ motion models) that a target can follow. The model indexed by $r=0$ is the stop model. The transition between the models is modelled as a Markovian process. In general when the target moves from one segment to the next, the set of dynamic models changes. In a conventional IMM estimator [15], [16], the likelihood function of a model i is given, for a track $\mathcal{T}^{k,l}$, associated with the j-th measurement, $j \in \{0,1,\ldots,m_k\}$ by:

$$\Lambda_k^i = p\{\mathbf{z}_k^j | M_k^{s,i}, Z^{k-1,n}\}, \quad i=0,1,\ldots,r \tag{16}$$

where $Z^{k-1,n}$ is the subsequence of measurements associated with the track $\mathcal{T}^{k,l}$.

Using the IMM estimator with a stop motion model, we get the likelihood function of the moving target mode for indexes $i \in \{0,1,\ldots,r\}$ and for $j \in \{0,1,\ldots,m_k\}$ by:

$$\Lambda_k^i = \quad P_D \cdot p\{\mathbf{z}_k^j | M_k^{s,i}, Z^{k-1,n}\} \cdot (1-\delta_{j,0}) + (1-P_D) \cdot \delta_{j,0} \tag{17}$$

The likelihood of the stopped target mode (*i.e.* $r=0$) is:

$$\Lambda_k^0 = p\{\mathbf{z}_k^j | M_k^{s,0}, Z^{k-1,n}\} = \delta_{j,0} \tag{18}$$

where $\delta_{j,0}$ is the Kronecker function defined by $\delta_{j,0}=1$ if $j=0$ and $\delta_{j,0}=0$ otherwise.

The combined (global) likelihood function Λ_k of a track including a stopped model is then given by:

$$\Lambda_k = \sum_{i=0}^{r} \Lambda_k^i \cdot \mu_{k|k-1}^i \tag{19}$$

where $\mu_{k|k-1}^i$ is the predicted model probabilities [15].

The steps of the IMM under road segment s constraint are the same as for the classical IMM

1) Step 1. Under the assumption of several possible models for segment s as defined previously, the mixing probabilities are given for $(i,l) \in \{0,1,\ldots,r\}^2$ by:

$$\mu_{k-1|k-1}^{i|l} = \frac{p_{il} \cdot \mu_{k-1}^i}{\bar{c}_l} \tag{20}$$

where $\bar{c}_l$ is a normalizing factor. The probability of model switch depends on the Markov chain according to the *a priori* transition probability p_{il} which does not depend on the constraint s.

2) Step 2. The mixed estimate of the target state under the road segment s constraint is defined for $i \in \{0, 1, \ldots, r\}$ by:

$$\hat{\mathbf{x}}^{0i,s}_{k-1|k-1} = \sum_{l=0}^{r} \mu^{i|l}_{k-1|k-1} \hat{\mathbf{x}}^{l,s}_{k-1|k-1} \tag{21}$$

The covariance of the estimation error is given by

$$\mathbf{P}^{0i,s}_{k-1|k-1} = \sum_{l=0}^{r} \mu^{i|l}_{k-1|k-1} \cdot [\mathbf{P}^{l,s}_{k-1|k-1} + (\hat{\mathbf{x}}^{l,s}_{k-1|k-1} - \hat{\mathbf{x}}^{0i,s}_{k-1|k-1}) \cdot (\hat{\mathbf{x}}^{l,s}_{k-1|k-1} - \hat{\mathbf{x}}^{0i,s}_{k-1|k-1})^{T}] \tag{22}$$

Despite of the constraint on local state estimates, the mixed state estimates do not belong to the road section s. That is why the optimized projection proposed in [1] is used to constrain the mixed estimate (21) and its associated covariance (22).

3) Step 3. The motion models are constrained to the associated road segment. Each constrained mixed estimate (21) is predicted and then associated to a new segment, or to several new ones (in crossroad case) which yields to the modification in the dynamics according to the new segments. The mixed estimates (21) and (22) are used as inputs for the filter matched to $\mathcal{M}^{i,s}$, which uses the MTI report associated to the track $\mathcal{T}^{k,l}$ to calculate $\hat{\mathbf{x}}^{i,s}_{k|k}$, $\mathbf{P}^{i,s}_{k|k}$ and the corresponding likelihood (19). The estimates of each filter are obtained with a constrainted Kalman filter (see [1] for more details).

4) Step 4. The model probability update is done for $i \in \{0, 1, \ldots, r\}$ by

$$\mu_i(k) = \frac{1}{c} \cdot \Lambda_i(k) \cdot \bar{c}_i \tag{23}$$

where c is a normalization coefficient and $\bar{c}_i$ is given in (20).

5) Step 5. The combined state estimate, called global state estimate, is the sum of each constrained local state estimate weighted by the model probability, *i.e.*

$$\hat{\mathbf{x}}_{k|k} = \sum_{i=0}^{r} \mu^{i}_{k} \hat{\mathbf{x}}^{i,s}_{k|k} \tag{24}$$

Here, one has presented briefly the principle of the IMM algorithm constrained to only one road segment s. However, a road section is composed with several road segments. When the target is making a transition from one segment to another, the problem is to choose the segments with

the corresponding motion models that can better fit the target dynamics. The choice of a segment implies the construction of the directional process noise. That is why the IMM motions model set varies with the road network configuration and Variable Structure Interacting Multiple Model (VS IMM) offers a better solution for ground target tracking on road networks as explained in next sections.

B. Variation of the set of constrained motion models

1) Variation on a road section: In the previous subsection, we have proposed a classical IMM with a given set of motion models. We have noted that the predicted state could give a local estimate under another road segment than the segment associated to the motion model (a road turn for example). The change to another road segment causes the generation of a new constrained motion models. In the literature, several approaches have been proposed to deal with the constrained motion models [17], [18]. In [1], we have proposed an approach to activate the most probable road segments sets. Based on the work of Rong Li [19], we consider $r+1$ oriented graphs which depend on the road network topology. For each graph i, $i = 0, 1, \ldots, r$, each node is a constrained motion model $\mathcal{M}^{i,s}$. The nodes are connected to each other according to the road network configuration. For instance, if we consider a road section R_h composed by three road segments s_1, s_2 and s_3, the i^{th} associated graph is composed by three nodes ($\mathcal{M}^{i,s_1}$, $\mathcal{M}^{i,s_2}$ and $\mathcal{M}^{i,s_3}$) where the nodes $\mathcal{M}^{i,s_1}$ and $\mathcal{M}^{i,s_3}$ are connected with the node $\mathcal{M}^{i,s_2}$. In [1], the activation of the motion model at the current time depends on the local constrained predicted state location of the track $\mathcal{T}^{k,l}$. In our example, the predicted constrained state belongs to the road segment s_1. So, we obtain $\hat{\mathbf{x}}^{i,s_1}_{k|k-1}$. The activation of the constraint motion model generates the constraint covariance matrix $\mathbf{P}^{i,s_1}_{k|k-1}$ according to the road segment location and road segment length (see section II-B). Consequently, we obtain a finite set of $r+1$ motion models constrained to a road section R_h (we recall that a road section is a set of connected road segments). Each local state is constrained on different road segments of the road section and several constrained motion models are activated.

2) Variation in a junction: However, an ambiguity arises when there are several road sections (*i.e.* when the target approaches a crossroad). In fact, the number of constrained motion models increases with the number of road sections present in the crossroad/junction. If we consider the $r+1$ graphs, the activation of the constraint motion model is done according to the predicted

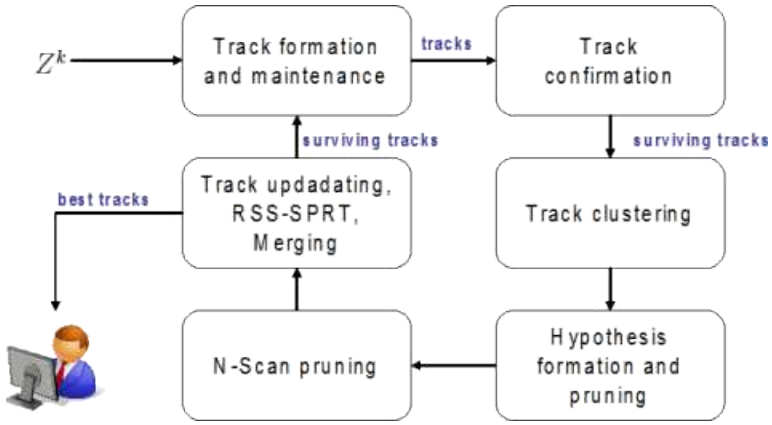

Figure 2: Structured-Branching Multiple Hypothesis Tracker (SB-MHT) logic flowchart with GIS.

states location. Consequently the number of motion models increases with the number of road sections. We obtain several constrained motion model sets. Each set is composed of $r + 1$ models constrained to road segments which belong to the road section. In order to select the most probable motion model set (*i.e.* in order to know on which road section the target is moving on), a sequential probability ratio test named Road Set Segment based on Sequential Probability Ratio Test (RSS SPRT) is proposed in [1] in order to select the road section taken by the target.

C. Multiple ground target tracker

We briefly describe here the main steps of the Variable Structure Interacting Multiple Model under Constraint (VS IMMC) Structured-Branching Multiple Hypothesis Tracker (SB-MHT). More details can be found in chapter 16 of [2].

1) The first functional block of the SB-MHT in figure 2 is the track confirmation and the track maintenance. When the new set Z^k of measurements is received, a standard gating procedure [2] is applied in order to determine the valid MTI reports to track pairings. The existing tracks are updated with VS IMMC and extrapolated confirmed tracks are formed. When the track is not updated with MTI reports, the stop-model is activated.

2) In order to palliate the association problem, we need a probabilistic expression for the evaluation of the track formation hypotheses that includes all aspects of the data association

problem. It is convenient to use the Log-Likelihood Ratio (LLR) or track score of a track $\mathcal{T}^{k,l}$ which can be expressed at current time k in the following recursive form [2]:

$$L_{k,l} = L_{k-1,n} + \Delta L_{k,l} \tag{25}$$

with

$$\Delta L_{k,l} = \log\left(\frac{\Lambda_k}{\lambda_{fa}}\right) \tag{26}$$

and

$$L(0) = \log\left(\frac{\lambda_{fa}}{\lambda_{fa} + \lambda_{nt}}\right) \tag{27}$$

where λ_{fa} and λ_{nt} are respectively the false alarm rate and the new target rate per unit of surveillance volume. Λ_k is the global likelihood function described in (19). After the track score calculation of the track $\mathcal{T}^{k,l}$, the Sequential Probability Ratio Test (SPRT) [20] is used to set up the track status either as deleted, tentative or confirmed track. The tracks that fail the SPRT are deleted and the surviving tracks are kept for the next stage.

3) The process of clustering is to put altogether the tracks that are linked by a common measurement. The clustering technique is used to limit the number of hypotheses to generate, and therefore to reduce the complexity of tracking system. The result of the clustering process is a list of tracks that are interacting. The next step is to form hypotheses of compatible tracks.

4) For each cluster, multiple coherent hypotheses are formed to represent the different compatible tracks scenarios. Each hypothesis is evaluated according to the track score function associated to the different tracks. Then, a technique is required to find the set of hypotheses set that represents the most likely tracks collection. The unlikely hypotheses and associated tracks are deleted by a pruning process and only the N_{Hypo} best hypotheses are conserved.

5) For each track, the *a posteriori* probability is computed and a classical *N-Scan* pruning approach [2] is used to select the confirmed and delete the most unlikely tracks. With this approach the most likely tracks are selected to reduce the number of tracks. However, the

N-Scan technique combined with the constraint implies that other tracks hypotheses (*i.e.* constrained on other road segments) are arbitrary deleted. To avoid this problem, we modify the *N-Scan* pruning approach in order to select the N_k best tracks on each N_k road sections.

6) Wald's SPRT proposed in section III-B is used to delete the unlikely hypotheses among the N_k hypotheses. The tracks are then updated and projected on the road network. In order to reduce the number of tracks to keep in the memory of the computer, a merging technique (selection of the most probable tracks which have common measurements) is also implemented.

D. Target type tracker

The target type tracker presented in [6] is used to improve the performance of the data association in the SB-MHT. The principle consists to update the posterior class probability vector at each scan time t_k, with the classifier output. After the refinement process presented in II-D, the classifier gives the probability vector $\beta_{k,l}$ of a track $\mathcal{T}^{k,l}$ given by :

$$\beta_{k,l} = \frac{P_J \otimes \beta_{k-1,n}}{P'_J \beta_{k-1,n}} \tag{28}$$

where P_J is the likelihood function of the subset J, $\beta_{k-1,n}$ is the prior probability provided by the previous updated track $\mathcal{T}^{k-1,n}$ and $\otimes$ is the Schur-Hadamard product. The initial classification vector is given by :

$$\beta_0 = P_J \tag{29}$$

In assuming the independence of the kinematic and classification observations, the augmented logarithm likelihood ratio $\Delta L^a_{k,l}$ for $\mathbf{z}_k^{MTI\star}$ or $\mathbf{z}_k^{UGS\star}$ defined respectively in (9) and (13) is the sum of the logarithm kinematic likelihood $\Delta L_{k,l}$ ratio given in (26) and the logarithm classification ratio $\Delta L^c_{k,l}$. The equation (25) is rewritten by

$$L_{k,l} = L_{k-1,n} + \Delta L^a_{k,l} \tag{30}$$

with

$$\Delta L^a_{k,l} = \Delta L_{k,l} + \Delta L^c_{k,l} \tag{31}$$

where $\Delta L_{k,l}$ is defined in (26).

The log-likelihood ratio of the classification belonging to the track $\mathcal{T}^{k,l}$ versus belonging to a false or new target is :

$$\Delta L^c_{k,l} = \log(\frac{P'_J \beta_{k-1,n}}{P'_J \beta_e}) \tag{32}$$

where e defines an extraneous target. If the track is not associated to a measurement at the current time t_k we have $\Delta L^c_{k,l} = 0$.

Finally the updated target type $\hat{c}_{k,l}$ of the track $\mathcal{T}^{k,l}$ is chosen as the maximum probability of updated classification vector (28). However, if this probability is not superior to 0.7, we use the taxonomy 2525C presented in the figure 1 to choose the target class that satisfies this condition. We calculate the probability of each node in the tree given the set $node = \{e_1, \ldots, e_n\}$ of n children nodes such that

$$P_{node} = P\{\bigcup_{i=i}^{n} e_i\} \tag{33}$$

The target class of a track $\mathcal{T}^{k,l}$ is obtained by taking the node that has a probability superior to 0.7:

$$\widehat{Class}_{k,l} = \{node, node \in \text{2525C}, P_{node} > 0.7\} \tag{34}$$

We remark that the first node "Ground Track" is always equal to one.

IV. Track segment association

A. Problem formulation

The goal of the Track Segment Association (TSA) is to reduce the number of broken tracks by using a correlation approach between tracks associated to the same target. In this first approach we do not consider the fusion of track segments based on feature element. We only consider an airborne GMTI sensor that gives MTI reports without Signal to Noise Ratio (SNR) or High Range Radial Resolution (HRRR) information. We recall that the MTI classification attributes are reduced to few elements and are not discriminant for the correlation function. So, to improve the TSA performances, we study a correlation function based on kinematics information and the track classification information updated with the UGS classification information.

In the multi-target tracking approaches, a data association algorithm (Multiple Hypothesis Tracker (MHT), Joint Probabilistic Data Association Filter (JPDAF), SD-Assignment, ...) is

used to associate measurements with predicted tracks in the presence of clutter. The problem is similar here because we try to associate a current track with an old track set in presence of false tracks (the tracker is not perfect and false tracks can appear in dense clutter area). Based on the works of [8], [21] on the track segment association, we propose an approach to solve the track segment association taking into account the road network and an IMM-smoother.

Two track sets are considered: an old track set $\mathcal{O}_k$ which contains the terminated track ("dead" or "stopped" tracks) at time t_k due to lack of measurement, and a current track set $\mathcal{C}_k$ which contains current updated tracks (the stop model is not activated) at time t_k.

The two sets $\mathcal{O}_k$ and $\mathcal{C}_k$ are updated at each sensor scan time by the following process:

1) Track sets selection. The first step is to build the tracks set $\mathcal{C}_k$ of current tracks and the tracks set $\mathcal{O}_k$.
2) Smoothing. The tracks contained in $\mathcal{O}_k$ and in $\mathcal{C}_k$ are smoothed.
3) Track correlation. On user's request or after a sliding window (in automatic mode), a retrodiction and prediction process are respectively done on tracks contained in $\mathcal{C}_k$ and old tracks contained in $\mathcal{O}_k$. At each scan time track segments are associated based on cost function.
4) Track assignment. The Auction algorithm [2] is used to solve the track segment association problem.

Each step of this TSA algorithm are detailed in the next sections

B. TSA Algorithm

1) Track sets selection: At each time t_k, the terminated and updated tracks are extracted from the tracker. An updated track $\mathcal{T}^{k,l}$ at the current time t_k is defined by the sequence of its estimated states and associated covariance. Its initialization time is noted $t_{k_i^l}$.

$$\forall \mathcal{T}^{k,l} \in \mathcal{C}_k, \quad \mathcal{T}^{k,l} \triangleq \{\hat{\mathbf{x}}^l_{t|t}, \mathbf{P}^l_{t|t}, t = k^l_i, \ldots, k\} \tag{35}$$

Starting from an empty set $\mathcal{C}_k$, the confirmed tracks are added to this one. In the set $\mathcal{O}_k$, there are all terminated tracks since the beginning of the surveillance mission. The deleted tracks $\mathcal{T}^{k_e^m,m}$, are defined with a termination time $t_{k_e^m}$ and a start time $t_{k_i^m}$. An old track is defined by

$$\forall \mathcal{T}^{k_e^m,m} \in \mathcal{O}_k, \quad \mathcal{T}^{k_e^m,m} \triangleq \{\hat{\mathbf{x}}^l_{t|t}, \mathbf{P}^l_{t|t}, t = k^m_i, \ldots, k^m_e\} \tag{36}$$

The times t_{k_e} and t_{k_i} are not necessarily the same for each track contained in $\mathcal{O}_{k-1}$. The current old track set $\mathcal{O}_k$ is based on the previous set $\mathcal{O}_{k-1}$ updated with the current deleted tracks. The tracks deleted by the SB-MHT at the current time t_k are added to set $\mathcal{O}_k$. In addition, to palliate the track discontinuity due to the stop-model activation we add to the set $\mathcal{O}_k$ the stopped tracks. If a stopped track present in $\mathcal{O}_{k-1}$ is moving at time t_k, it is extracted from $\mathcal{O}_k$ and added to $\mathcal{C}_k$. In our simulation, a track is declared as "stopped" if the confirmed track has a stop-model probability greater than 0.9. The cardinality of the sets $\mathcal{C}_k$ and $\mathcal{O}_k$ are not necessarily the same.

2) IMM fixed-lag smoother: The Interacting Multiple Model (IMM) estimator presented in this paper has been proven to be effective for tracking maneuvering ground targets with a GMTI sensor. This is more significant if the contextual information is taking into account in the tracking process. For intelligent system, the real-time application for tactical situation establishment is primordial. The second main point is to understand the situation assessment in constrained time. So we can use this time period to achieve the best estimates of the target states at a given time based on all measurements up to the current time. In addition, the achievement process contributes to improve the initial estimated state and consequently the track retrodiction precision.

For this, we must take into account all the measurements of a track available in a sliding window. According to the IMM estimator, we use a Rauch Tung Striebel (RTS) IMM smoothing algorithms presented in [22], [23] which involves forward filtering followed by backward smoothing. The forward recursion is performed using the VS IMMC algorithm. The backward recursion keeps the selected model set of the track and imitates the IMM estimator in the forward direction. In this subsection we describe the IMM smoothing method presented in [22], [23]. In addition we use the smoothing step to constraint the past of the current tracks to belong to the road network when possible.

a) Interacting Multiple Model Smoother: The steps of the smoothing method for multiple approach are briefly presented here. In the backward smoothing, we calculate the smoothed state at time t_t given the measurement up to time t_k, considering the length L of a sliding window, where $t_{k-L} \leq t_t \leq t_k$. As for the IMM forward recursion, the IMM backward recursion consists of four parts: mode probability calculation, mixing, smoothing and combination.

- Mode probability calculation: the backward transition probability π is computed by $\forall(i,j) \in$

$\{1,\ldots,r\}^2$:

$$\pi_{ij} = \frac{p_{ji}\mu^j_{t|t}}{c_i} \tag{37}$$

where

$$c_i = \sum_{l=1}^{r} p_{li}\mu^l_{t|t} \tag{38}$$

- Mixing: the backward mixing probability is computed by $\forall(i,j) \in \{1,\ldots,r\}^2$:

$$\mu^{i|j}_{t+1|k} = \frac{\pi_{ij}\mu^i_{t+1|k}}{d_j} \tag{39}$$

where

$$d_j = \sum_{l=1}^{r} \pi_{lj}\mu^l_{t+1|k} \tag{40}$$

The smoothed state of the i^{th} motion model and its associated covariance are given by:

$$\hat{\mathbf{x}}^{0i,s}_{t+1|k} = \sum_{i=1}^{r} \mu^{i|j}_{t+1|k}\hat{\mathbf{x}}^{i,s}_{t+1|k} \tag{41}$$

$$\mathbf{P}^{0i,s}_{t+1|k} = \sum_{i=1}^{r} \mu^{i|j}_{t+1|k}\{\mathbf{P}^{i,s}_{t+1|k} + \left[\hat{\mathbf{x}}^{i,s}_{t+1|k} - \hat{\mathbf{x}}^{0i,s}_{t+1|k}\right]\left[\hat{\mathbf{x}}^{i,s}_{t+1|k} - \hat{\mathbf{x}}^{0i,s}_{t+1|k}\right]^T\} \tag{42}$$

- Model-Smoothing: according to the RTS recursive formula [22], [23], the smoothing equations for each motion model i are given by:

$$\hat{\mathbf{x}}^{i,s}_{t|k} = \hat{\mathbf{x}}^{i,s}_{t|t} + C^i_t(\hat{\mathbf{x}}^{0i,s}_{t+1|k} - \hat{\mathbf{x}}^{i,s}_{t+1|t}) \tag{43}$$

$$\mathbf{P}^{i,s}_{t|k} = \mathbf{P}^{i,s}_{t|t} + C^i_t(\mathbf{P}^{0i,s}_{t+1|k} - \mathbf{P}^{i,s}_{t+1|t})C^{i^T}_t \tag{44}$$

where $\hat{\mathbf{x}}^{i,s}_{t+1|t}$ and $\mathbf{P}^{i,s}_{t+1|t}$ are the predicted state and covariance corresponding to the i^{th} model and C^i_t is the smoothing gain given by :

$$C^i_t = \mathbf{P}^{i,s}_{t|t}\mathbf{F}^{i,s^T}_t(\mathbf{P}^{i,s}_{t+1|t})^{-1} \tag{45}$$

The estimated states and covariances are constrained to the road segment associated with the constraint motion model $\mathcal{M}^{i,s}$.

- Combination: the smoothed mode probability is defined by:

$$\mu^j_{t|k} = \frac{\Lambda^j_{t|k}}{c}\mu^j_{t|t} \tag{46}$$

where the normalizing constant c is equal to

$$c = \sum_{i=1}^{r} \Lambda_{t|k}^{i} \mu_{t|t}^{j} \tag{47}$$

and

$$\Lambda_{t|k}^{j} = \sum_{i=1}^{r} p_{ji} \mathcal{N}(\hat{\mathbf{x}}_{t+1|k}^{i,s}; \hat{\mathbf{x}}_{t+1|t}^{i,s}, \mathbf{P}_{t+1|t}^{i,s}) \tag{48}$$

Finally, the smoothed state and its associated covariance matrix are given by:

$$\hat{\mathbf{x}}_{t|k}^{s} = \sum_{i=1}^{r} \mu_{t|k}^{i} \hat{\mathbf{x}}_{t|k}^{i,s} \tag{49}$$

$$\mathbf{P}_{t|k}^{s} = \sum_{i=1}^{r} \mu_{t|k}^{i} \{\mathbf{P}_{t|k}^{i,s} + [\hat{\mathbf{x}}_{t|k}^{i,s} - \hat{\mathbf{x}}_{t|k}^{s}][\hat{\mathbf{x}}_{t|k}^{i,s} - \hat{\mathbf{x}}_{t|k}^{s}]^{T}\} \tag{50}$$

b) On-road track correction: After the smoothing process the constrained tracks are always on the road network, but some unconstrained tracks can also belong to the road network. For each unconstrained smoothed state we use the statistical test presented in [11] to project the smoothed states and their covariances on the most probable road segment.

3) Track correlation:

a) Retrodiction and association: The retrodiction is the backward prediction of each track contained in $\mathcal{C}_k$. From each starting time $t_{k_i^l}$ of each track $\mathcal{T}^{k,l}$, we use a back propagation equation of a constant velocity motion model given in (2). For each track $\mathcal{T}^{k,l}$, a sequence of retrodicted states is obtained at previous times for each deleted tracks of $\mathcal{O}_k$. The set of candidate track pairs for TSA is obtained according a two-step validation procedure:

1) The first step of tracks pairing consists of a velocity gating. As illustrated in the figure 3, we associate the current track with old tracks if the maximum ground target speeds are below v_{max}. The set of pairing tracks satisfying this condition is defined by

$$\begin{aligned} \Phi_v = \{(\mathcal{T}^{k_i^l,l}, \mathcal{T}^{k_o,m}) \text{ such that } \frac{|\hat{x}_{k_c|k_i^l}^{l} - \hat{x}_{k_c|k_o}^{m}|}{t_{k_i} - t_{k_o}} \leq v_{max}, \frac{|\hat{y}_{k_c|k_i^l}^{l} - \hat{y}_{k_c|k_c}^{m}|}{t_{k_i} - t_{k_o}} \leq v_{max}, \\ \mathcal{T}^{k,l} \in \mathcal{C}_k, \mathcal{T}^{k_o,m} \in \mathcal{O}_k, t_{k_i^m} < t_{k_o} < t_{k_e^m}, t_{k_c} = \frac{t_{k_i^l} - t_{k_o}}{2}\} \end{aligned} \tag{51}$$

where $(\hat{x}_{.|k_i^l}^{l}, \hat{y}_{.|k_i^l}^{l})$ is the retrodicted location of the track $\mathcal{T}^{k,l}$ and $(\hat{x}_{k_c|k_o}^{m},\ \hat{y}_{k_c|k_o}^{m})$ is the predicted location of the track $\mathcal{T}^{k_o,m}$ as described in II-B.

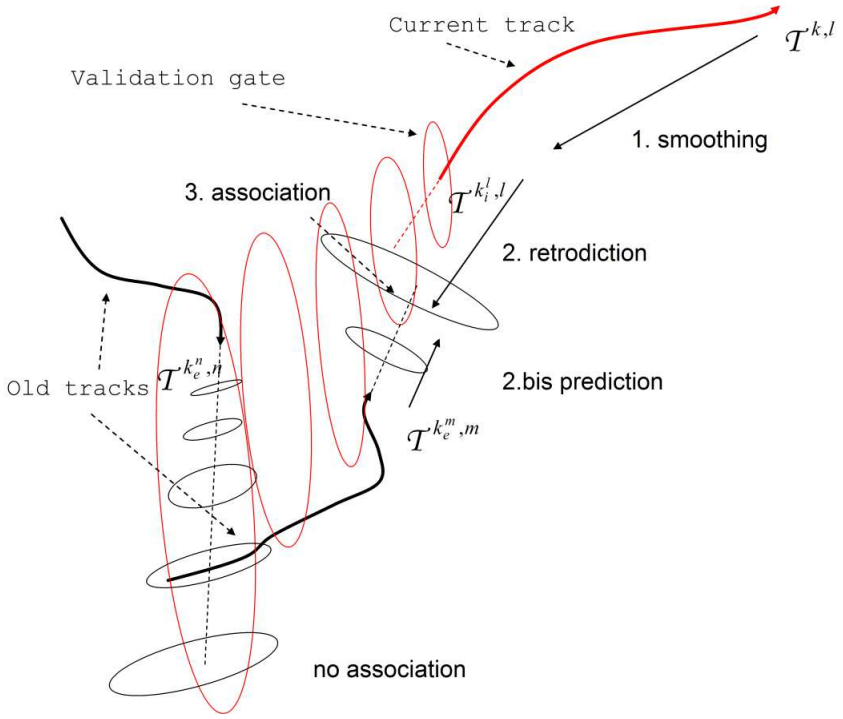

Figure 3: Track segment association principle.

This is the approach used in [8] where the track pairing of the old track $\mathcal{T}^{k_e^m,m}$ is done at each time $\{t_{k_i^m}, \ldots, t_{k_e^m}\}$ and not only at the time end $t_{k_e^m}$.

2) The second step is done to limit the number of track pairings. Under the statistical noise independence between the current tracks of $\mathcal{C}_k$ and the old tracks $\mathcal{O}_k$, we use a classical χ^2_n test (n, the state vector dimension, is the degree of freedom) to validate the pairs in Φ_v. At time t_{k_c} the difference between the retrodicted tracks of $\mathcal{T}^{k_i^l,l}, (\mathcal{T}^{k,l} \in \mathcal{C}_k)$ and predicted tracks of $\mathcal{T}^{k_o,m}, (\mathcal{T}^{k_e^m,m} \in \mathcal{O}_k)$ is defined by:

$$\Delta^{l,m}_{k_c} = \hat{\mathbf{x}}^l_{k_c|k_i^l} - \hat{\mathbf{x}}^m_{k_c|k_o} \tag{52}$$

with the covariance:

$$\mathbf{P}^{l,m}_{k_c} = \mathbf{P}^l_{k_c|k_i^l} - \mathbf{P}^m_{k_c|k_o} \tag{53}$$

The new set of track pairing candidate is defined by the following statistical test:

$$\begin{aligned}\Phi_s = \{(\mathcal{T}^{k_i^l,l}, \mathcal{T}^{k_o,m}) \mid (\Delta^{l,m}_{k_c})^T [\mathbf{P}^{l,m}_{k_c}]^{-1} (\Delta^{l,m}_{k_c}) \leq \chi^2_n(1-Q),\\ (\mathcal{T}^{k_i^l,l}, \mathcal{T}^{k_o,m}) \in \Phi_v, t_{k_i^m} < t_{k_o} < t_{k_e^m}, t_{k_c} = \frac{t_{k_i^l} - t_{k_o}}{2}\}\end{aligned} \tag{54}$$

where Q is a fixed tail probability. The counterpart of this approach is in the set Φ_s, where several pairs can correspond to the same tracks pairing between $\mathcal{T}^{\cdot,l}, (\mathcal{T}^{k,l} \in \mathcal{C}_k)$ and $\mathcal{T}^{\cdot,m}, (\mathcal{T}^{k_e^m,m} \in \mathcal{O}_k)$. In order to limit the complexity in the assignment algorithm we keep the pairs which have the minimal statistical distance among all pairs of the same tracks.

b) Track assignment: After applying the gating (54), we obtain a set of track pairs candidates between current track in $\mathcal{C}_k$ and deleted or stopped tracks in $\mathcal{O}_k$. The association is formulated as a 2-D assignment problem. For this, we define a binary assignment variable as

$$a(\mathcal{T}^{k_i^l,l}, \mathcal{T}^{k_o,m}) = \begin{cases} 1 & \text{track } \mathcal{T}^{k_i^l,l} \text{ is originated from the track } \mathcal{T}^{k_o,m} \text{ at time } t_{k_o} \\ 0 & \text{otherwise.} \end{cases} \tag{55}$$

The cost of the track association between $\mathcal{T}^{k_i^l,l}$ and $\mathcal{T}^{k_o,m}$ is denoted by $c(\mathcal{T}^{k_i^l,l}, \mathcal{T}^{k_o,m})$, and is defined by

$$c(\mathcal{T}^{k_i^l,l}, \mathcal{T}^{k_o,m}) = \begin{cases} -\log \frac{\mathcal{N}(\Delta_{k_c}^{l,m}; 0, \mathbf{P}_{k_c}^{l,m})}{\mu} & \text{if } (\mathcal{T}^{k_i^l,l}, \mathcal{T}^{k_o,m}) \in \Phi_s \\ -\log(1 - P_{D_s}) & \text{otherwise.} \end{cases} \tag{56}$$

where μ is given by the spatial density of the extraneous tracks in the state space and P_{D_s} is the probability that a target is tracked [8].

The optimal set of track pairs (optimal assignment) is obtained by minimizing the following global cost C:

$$C = \sum_{l=1}^{M_c} \sum_{m=1}^{N_o} a(\mathcal{T}^{k_i^l,l}, \mathcal{T}^{k_o,m}) c(\mathcal{T}^{k_i^l,l}, \mathcal{T}^{k_o,m}) \tag{57}$$

under the constraints:

$$\sum_{l=1}^{M_c} a(\mathcal{T}^{k_i^l,l}, \mathcal{T}^{k_o,m}) = 1, m = 1, \ldots, N_o \tag{58}$$

$$\sum_{m=1}^{N_o} a(\mathcal{T}^{k_i^l,l}, \mathcal{T}^{k_o,m}) = 1, l = 1, \ldots, M_c \tag{59}$$

where M_c and N_o are respectively the number of current associated tracks and the number dead associated tracks. This 2-D assignment problem is solved using the Auction algorithm [2].

c) Track segment association algorithm execution: In our application, the track segment association algorithm is applied every minute. The track retrodiction is done for each current track after the smoothing process. We use the validation tests to determine the cost between current track segment and dead track segments. A new current track segment is obtained after the TSA algorithm. A dead track at the current time t_k is extracted from the set $\mathcal{O}_k$ if it is not used for the track segment association during two minutes.

C. Introduction of the target type information in the TSA algorithm

We propose also to introduce the track classification information in the Track Segment Association (TSA) process in order to increase the discrimination between the old and current tracks. Two methods are presented for such purpose.

1) Track classification gating: this first method is the easiest. We propose to add a new test in the track pairing test (54). This test consists to validate only the track with the same classification level between a current track $\mathcal{T}^{k,l}$ and a old track $\mathcal{T}^{k_e^m,m}$. So, we add the following new condition in (54)

$$\widehat{Class}_{k,l} = \widehat{Class}_{k_e^m,m} \tag{60}$$

Remark: it is more efficient to choose the updated type at the current time t_k for the track $\mathcal{T}^{k,l}$ even if the kinematic test is done on the initial smoothed state at time $t_{k_i^l}$.

2) Track classification scoring: the second method consists to modify the cost association presented in (56) by introducing a track classification cost. After the pairing test (54) between the current track $\mathcal{T}^{k,l}$ and the old track $\mathcal{T}^{k_e^m,m}$, the track class vectors $\beta_{k_i^l,l}$ and $\beta_{k_e^m,m}$ are compared based on the Bhattacharyya distance:

$$c(\beta_{k,l}, \beta_{k_e^m,m}) = -\log \sum \sqrt{\beta_{k,l} \cdot \beta_{k_e^m,m}} \tag{61}$$

The global cost association becomes:

$$c(\mathcal{T}^{k_i^l,l}, \mathcal{T}^{k_o,m}) = \begin{cases} -\log \frac{\mathcal{N}(\Delta_{k_c}^{l,m};0,\mathbf{P}_{k_c}^{l,m})}{\mu} + c(\beta_{k,l}, \beta_{k_e^m,m}) & \text{if } (\mathcal{T}^{k_i^l,l}, \mathcal{T}^{k_o,m}) \in \Phi_s \\ -\log(1 - P_{D_s}) & \text{otherwise.} \end{cases} \tag{62}$$

V. Simulation and results

In this paper, we evaluate the impact of the classification information introduced in the TSA algorithm for multiple ground target tracking. The results presented are based on a Monte-Carlo simulation with 100 runs.

A. Measures of performance

Several Measures Of Performance (MOP) have been used in simulations to evaluate our approach for the Track Segment Association (TSA) algorithm. Each confirmed track is associated to at most one target. For this, we calculate the error at each scan time between the trajectory of the targets and the confirmed track and if this error is less than $30m$ we associate the track to the target that has the shortest error in distance. A confirmed track is obtained after the track confirmation level in the SB-MHT.

1) Track Segment Purity (TSP) measures the correct association between a track and a measure of the target. This measure is directly averaged by the number N of tracks associated to the same target. Mathematically, TSP is defined by

$$\text{TSP} = \frac{1}{N}\sum_{l=1}^{N} n(\mathcal{T}^{k,l})/n_T \tag{63}$$

where $n(\mathcal{T}^{k,l})$ is the number of measurements of the track $\mathcal{T}^{k,l}$ generated by the target associated to the track, n_T is the number of measurements in the track $\mathcal{T}^{k,l}$.

2) Mean Track Life (MTL) measures the track continuity. If the MTL of a target is near to one, we can conclude that the target is well tracked. This MOP is directly averaged by the number N of tracks associated to the same target. Mathematically, the MTL is defined by

$$\text{MTL} = \frac{1}{N}\sum_{l=1}^{N} l(\mathcal{T}^{k,l})/l_T \tag{64}$$

where $l(\mathcal{T}^{k,l})$ is length of the track $\mathcal{T}^{k,l}$ associated to the target, and l_T is the length of the target trajectory.

3) Percentage of Correct Classification (PCC) measures is the third MOP used in this work to evaluate this new TSA method. To calculate the PCC we observe at each scan time the updated class given by the relation (34). We sum at each scan time the class of the track similar to the class of the target divided by the track length. This measure is directly averaged by the number N of tracks associated to the same target. Mathematically, the PCC is defined by

$$\text{PCC} = \frac{1}{N}\sum_{l=1}^{N} n_c(\mathcal{T}^{k,l})/l_{\mathcal{T}^{k,l}} \tag{65}$$

where $n_c(\mathcal{T}^{k,l})$ is the number of correct classification of the track $\mathcal{T}^{k,l}$ associated to a target and $l_{\mathcal{T}^{k,l}}$ is the length of tre track $\mathcal{T}^{k,l}$.

B. Scenario description

The scenario duration is limited to 10 minutes.

1) Targets description: We consider 20 targets that are able to maneuver (acceleration, deceleration, stop), pass and cross the others targets. The relations between target type, the target classification set and the taxonomy 2525C are given in the table I. We recall that the frame of discernment C_{UGS} is similar to C_{2525C}. In figure 4, we present the target trajectories at different time.

Target	Target type	Target class in C_{MTI}	Target class in C_{2525C}
1	TWINGO	Wheeled	Compact Automobile
2	Citroen xsara	Wheeled	Midsize Automobile
3	Small Bus	Wheeled	Small Bus
4	Renault Scenic	Wheeled	Sedan Automobile
5	Peugeot 206	Wheeled	Compact Automobile
6	Laguna II	Wheeled	Midsize Automobile
7	Van	Wheeled	Van
8	Large Bus	Wheeled	Large Bus
9	4x4 TOYOTA	Wheeled	Jeep Medium
10	civilian heavy truck	Wheeled	Large Box Truck
11	Midsize Bus	Wheeled	Small Bus
12	civilian heavy truck	Wheeled	Large Box Truck
13	VBL	Wheeled	Light Wheeled
14	VAB	Tracked	Medium Tracked
15	VAB	Tracked	Medium Tracked
16	Renault Scenic	Wheeled	Sedan Automobile
17	AMX-30	Tracked	Heavy Tracked
18	AMX-30	Tracked	Heavy Tracked
19	TWINGO	Wheeled	Compact Automobile
20	Military Van	Wheeled	Bus

Table I: Correspondence between target type and target classification in C_{MTI} and C_{2525C}.

2) Sensor parameters: The GMTI sensor is located at $(-40km, 40km)$ in the TCF and is moving at $5km$ in altitude according a trajectory represented on the figure 5. The sampling period is fixed at $0.25Hz$ (*i.e.* 4 seconds), the azimuth standard deviation is $0.001rad$, the range standard deviation is $10m$ and the range rate standard deviation is $1m.s^{-1}$. The detection

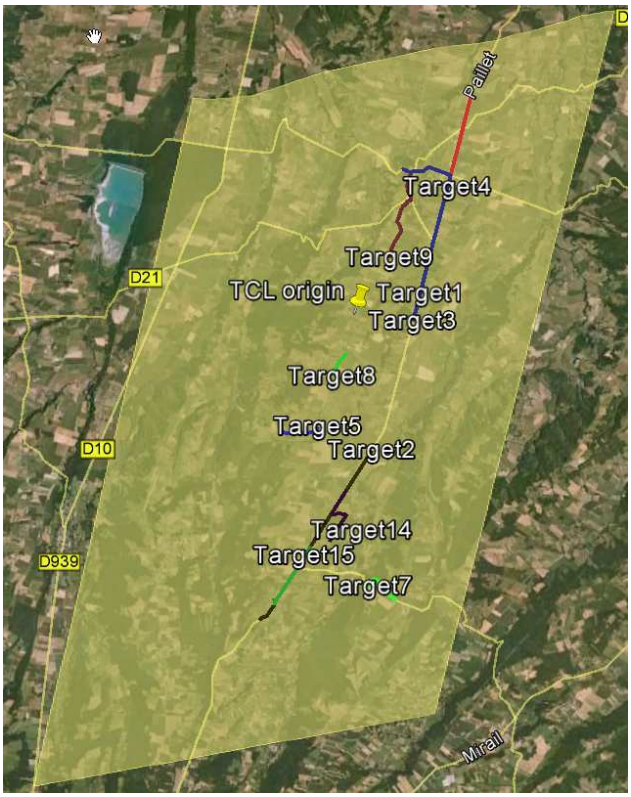

(a) Location of the targets at time 184 s.

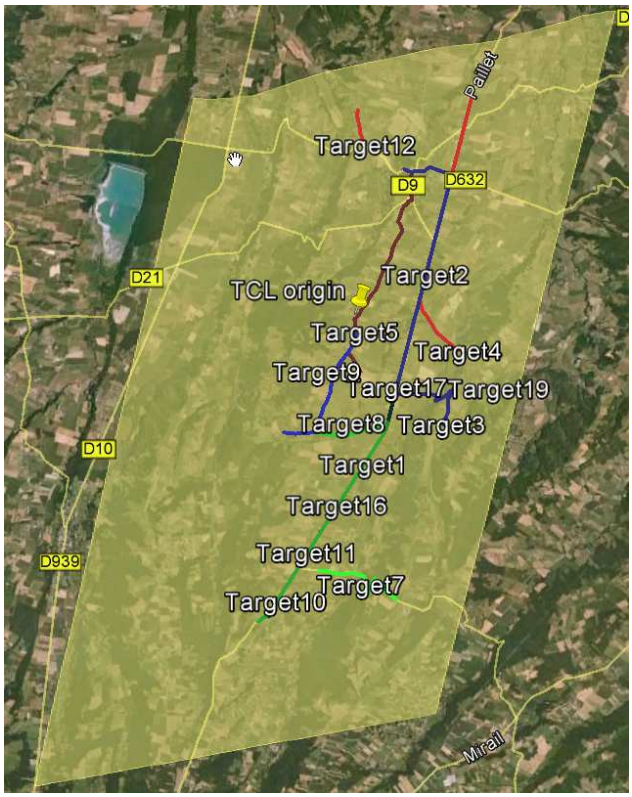

(b) Location of the targets at time 349 s.

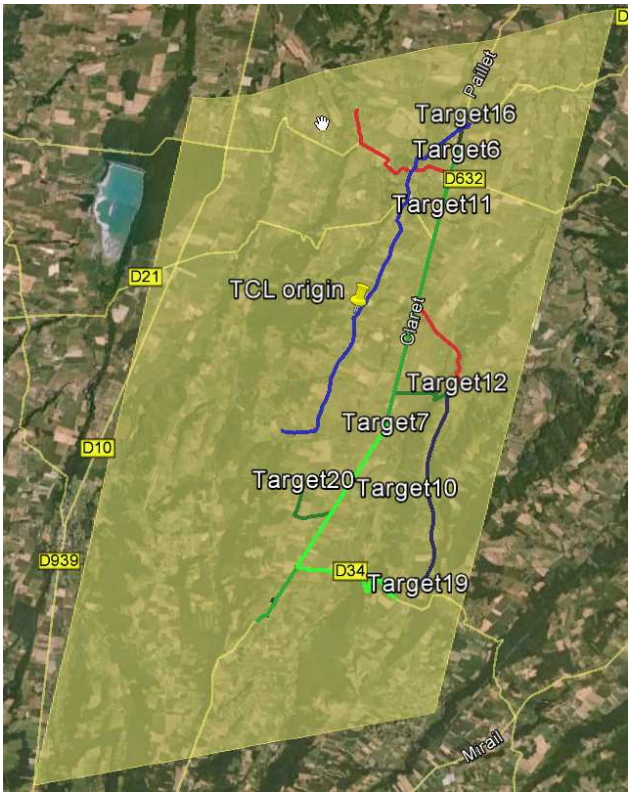

(c) Location of the targets at time 540 s.

Figure 4: Screen shots of the target's location.

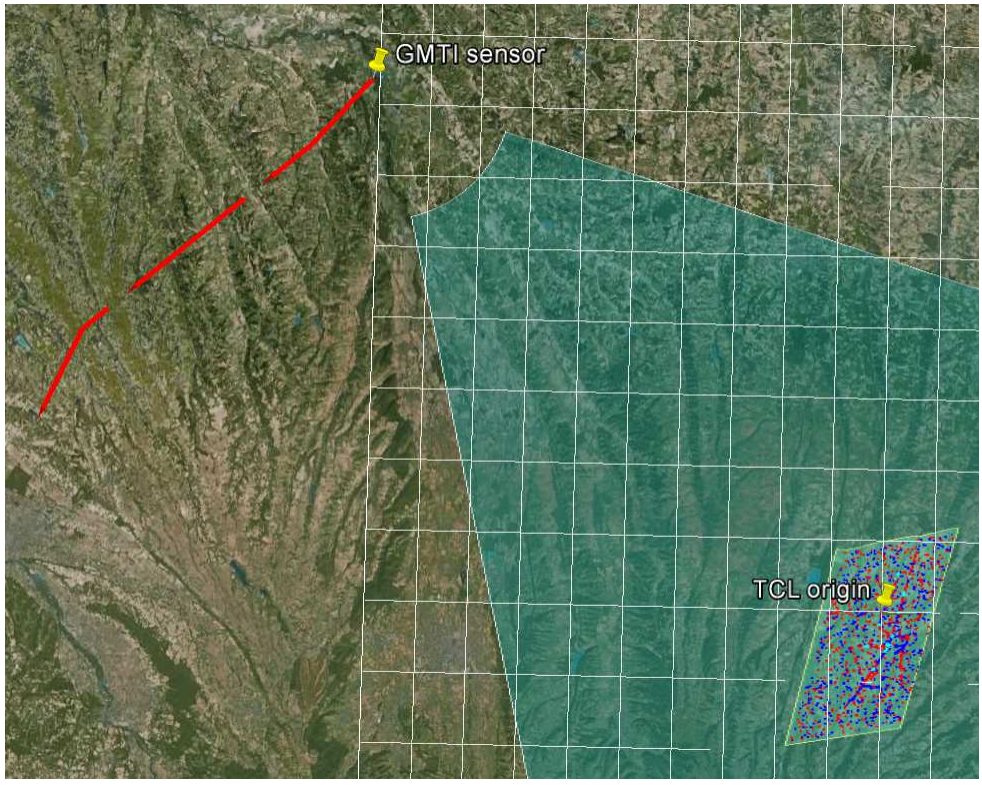

Figure 5: GMTI sensor trajectory. The red segments are the activated sensor location, the cyan area is the sensor coverage, the yellow parallelogram is the area of interest, the red and blue dots are the MTI reports with positive and negative radial velocity.

probability is fixed to 0.9 with a Minimal Detectable Velocity (MDV) equal to $1m.s^{-1}$. The false alarm probability is equal to 10^{-7}. The confusion matrix of each class of C_{MTI} is

$$\mathbf{C}_k = \begin{pmatrix} 0.8 & 0.1 & 0.1 \\ 0.15 & 0.7 & 0.15 \\ 0.05 & 0.05 & 0.9 \end{pmatrix} \tag{66}$$

The figure 6 represents the cumulated MTI reports over the time scenario (*i.e.* 10 minutes). In order to simulate the cut-off of the GMTI sensor during its maneuvers, we consider that every 3 minutes, the UAV changes its trajectory and cut-off the GMTI sensor during 40 seconds.
The parameters of the UGS are simplified and characterized by a standard deviation equal to $2m$, a false alarm probability fixed to 10^{-9}, and a sampling time fixed to $1Hz$. The location and the sensor area coverage are given on the figure 7 and 8 respectively. The UGS are always

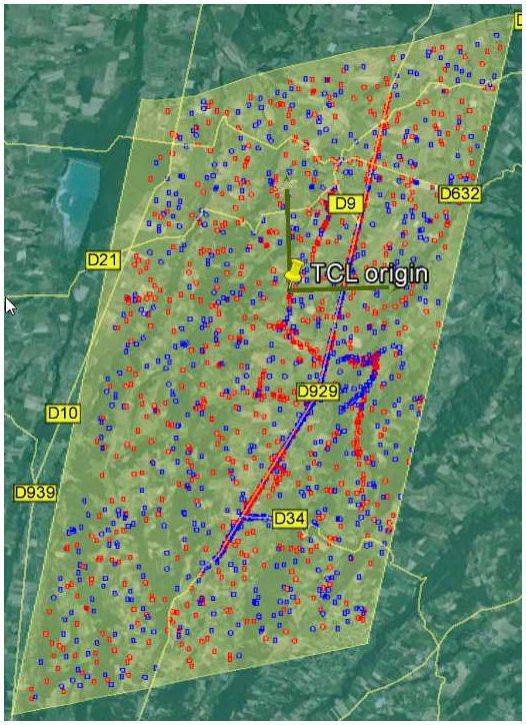

Figure 6: Cumulated MTI reports. The red and blue dots are the MTI reports with positive and negative radial velocity.

activated. Each detection is provided with the diagonal element of the confusion matrix C_{UGS} equal to 0.8. The other terms of the column are equi-distributed in the manner that the sum without the diagonal element is equal to 0.2.

The sensor activation or desactivation time and the presence time of the targets are represented in the figure 9.

3) Filter parameters: We have used VS IMMC SB-MHT for multiple target tracking. The parameter settings are given as follows:

a) VS IMMC parameters: The motion models are constant velocity motion models. A motion model $\mathcal{M}^{s,1}$ to track the targets which move with constant velocity on the road, a motion model $\mathcal{M}^{s,2}$ with a big state noise to palliate the maneuvers of the target and a stop-model $\mathcal{M}^{s,0}$. The noises of the previous motion models are the following :$\sigma_d = 0.1m.s^{-2}$, $\sigma_n = 0.1m.s^{-2}$ for $\mathcal{M}^{s,1}$, $\sigma_n = 1m.s^{-2}$, $\sigma_n = 0.5m.s^{-2}$ for $\mathcal{M}^{s,2}$ and $\sigma_d = 0.1m.s^{-2}$, $\sigma_n = 0.05m.s^{-2}$ for $\mathcal{M}^{s,0}$. For the unconstrained motion models $\mathcal{M}^1$, $\mathcal{M}^2$ and $\mathcal{M}^0$, we use the noises with

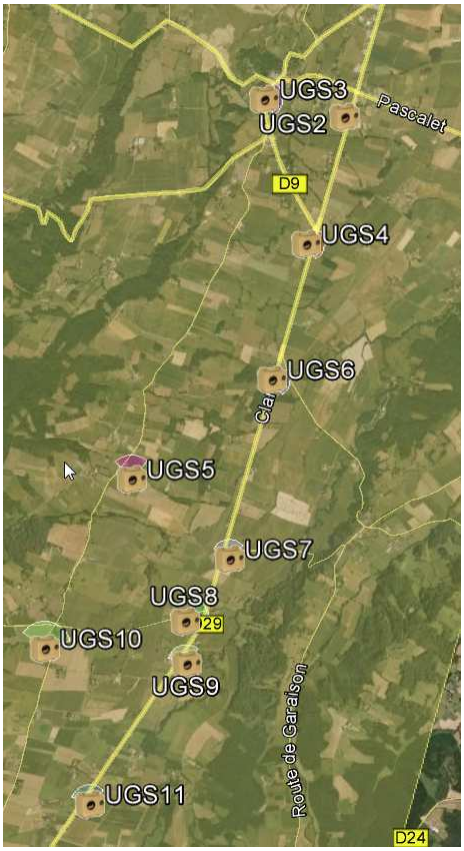

Figure 7: Location of the UGS.

Figure 8: Screen shot of the cumulated reports of the UGS 7, 8, 9 and 10.

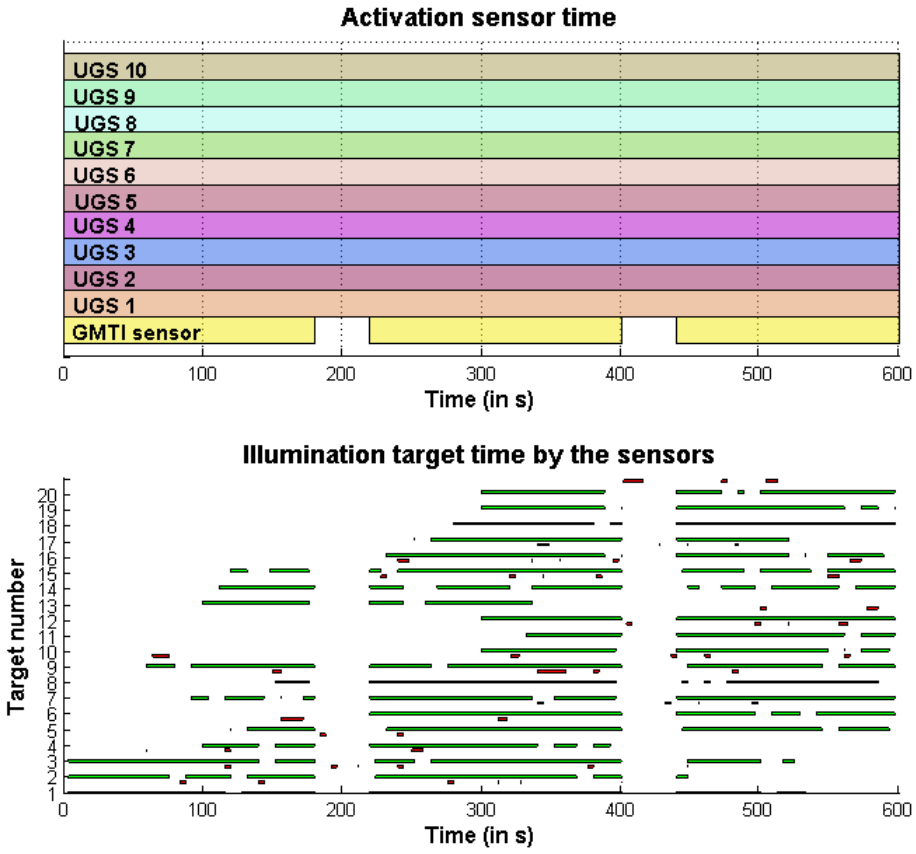

Figure 9: Sensor activation time and illumination target time by the sensors. The green time slot is associated to the GMTI sensor and the red time slot is associated to the set of UGS.

$\sigma = 0.1m.s^{-2}$, $\sigma = 2m.s^{-2}$ and $\sigma = 0.5m.s^{-2}$ respectively. The initial model probabilities and transition probability matrix were

$$\mu(0) = [0.9\ 0.1\ 0]^T \tag{67}$$

$$\pi = \begin{pmatrix} 0.9 & 0.095 & 0.005 \\ 0.3 & 0.65 & 0.15 \\ 0.1 & 0.6 & 0.3 \end{pmatrix} \tag{68}$$

b) SB-MHT parameters:

- For the track initialisation: each MTI report at every scan is considered as a new track. The initialised track is declared as “tentative track”. The MTI reports are validated with a

classical gating procedure (a Chi2 test with a probability of gating equal to $P_g = 0.95$).

- For the track termination step, a track is declared as "deleted track" if the probability of the stop-model is greater than 0.9, and if the track is not associated to measurements during $30seconds$.
- For the track association step: a track is associated to a report if the MTI report is validated according the previous test (with a gating probability equal to $P_g = 0.95$ for unconstrained tracks and $P_g = 0.99$ for constrained tracks), and if the maximum velocity allowed for a ground target is less than $35m.s^{-1}$.
- In the hypothesis generation step of the MHT: the threshold used to keep a track hypothesis is fixed to 0.01, and the track is maintained if its global track probability is greater than 0.1. The number of scans before the N-Scan pruning process is equal to 3.
- For the TSA algorithm, the smoothing process is realized every minute.

C. Results

To evaluate the impact of the classification information introduced in the TSA algorithm, we test the VS IMMC SB-MHT with three TSA versions: the first version is a TSA algorithm without classification information represented in red color, the second version is a TSA algorithm including the classification distance in the cost function (presented in IV-C2) represented in blue color, and the third version is a TSA algorithm including the classification gating procedure (presented in IV-C1) represented in yellow color. We recall the results are based on a 100 runs Monte-Carlo simulation.

The figure 10 represents the average MTL of each target. We observe that globally the introduction of classification information improves the performance of the track segment association algorithm because the length of tracks with respect to the length trajectory of the associated target is greater with the classification information (blue and yellow bars) than without (red bars). We observe also a large difference of performances between the tracks associated to the targets 19 and 20. This difference is due to the UGS illumination of the targets. In fact, the UGS provide a better classification information and the target 20 is illuminated by this sensor type during 15 seconds. According the UGS sampling time, the illumination duration is very sufficient to obtain a good and precise estimation of the class. The target 19 is never illuminated by the UGS sensor but it evolves at the proximity of the target 20. So, when the TSA algorithm

is executed, the targets 19 and 20 are well discriminated in class information. A similar remark applies for the targets that have a correct class estimator due to a long illumination time by UGS sensors. However, the gating procedure doesn't take into account the sensor type uncertainty. We reveal also the limits of the gating procedure because the MTL of the TSA algorithm with the gating procedure is inferior to TSA algorithm with the scoring procedure. In addition, the table II shows the TSP and PCC of tracks associated to each target. Introduction of the classification information improves the association between tracks and measurements originated from the corresponding target. In fact, the TSP of the TSA algorithm without class information is inferior to the TSA algorithms with scoring and gating class information expected for the targets 16, 19 and 20. The TSP values for those targets are higher than TSP values with scoring technique. This phenomenon is due to bad classification results because the target type is not discriminant, or because the targets are not illuminated sufficiently by a UGS. The introduction of the class cost decreases the performances of the TSA algorithm if the class likelihood can't select the good class or discriminate the targets in the same cluster. So, if an ambiguity occurs on the track class, or if the tracks are not illuminated by UGS we recommend to not use the class information in the cost function, otherwise the TSA performances will degrade.

VI. Conclusions

We have presented a complete process to track multiple ground targets with airborne GMTI sensors. The first step is to track maneuvering targets in a complex ground environment with the only information in target location and range radial velocity. We have proposed, in the first part, to adapt the Interacting Multiple Model (IMM) algorithm by taking into account the road network and the Structured-Branching Multiple Hypothesis Tracker (SB-MHT) to obtain several association scenarii in road intersection. In this paper, we focus on the Track Segment Association (TSA) algorithm in order to associate the track segments obtained by after several fly paths. In fact, when the airborne GMTI sensors observes an area of interest, the Unnamed Aerial Vehicle (UAV) maneuvers after few minutes to obtain a new trajectory in order to conserve its capacity to observe its surveillance area. During the maneuvers and due to sensor constraint the GMTI sensor is shut down. The tracker is reinitialized to avoid track association errors. To improve the track continuity we have studied and developed a Track Segment Association (TSA) algorithm. However, due to the ground targets density and targets proximity, the Track

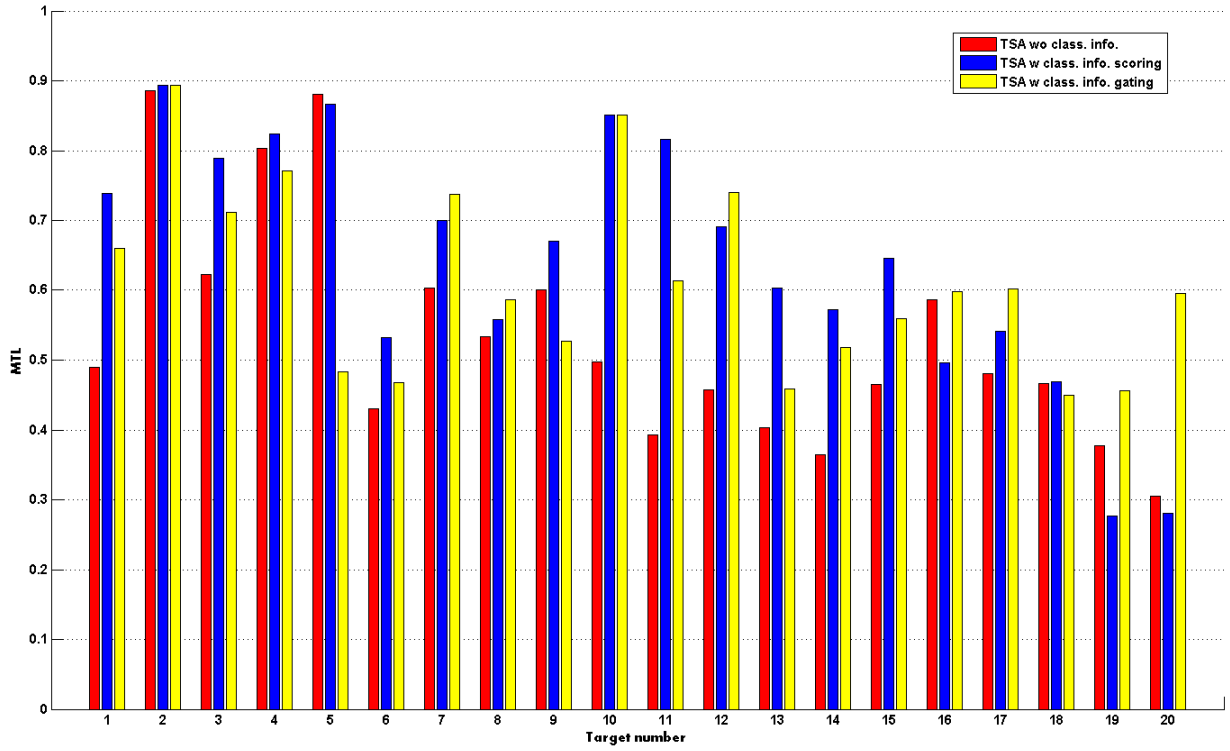

Figure 10: Mean Track Life (MTL) of each target.

Segment Association (TSA) algorithm is perfectible because the cost function is based only on kinematic information. That is why it appears interesting to deploy Unattended Ground Sensor (UGS) sensors and to develop methods to deal with the uncertain and imprecise identification information of the observed target. We have proposed to modelize the classification information for each sensor type and introduce the classification information in the log-likelihood function in the Structured-Branching Multiple Hypothesis Tracker (SB-MHT) and also in the cost function of the Track Segment Association (TSA) algorithm. Our results show that the introduction of classification improves the track segment association and the track continuity between several fly paths whenever the target are well illuminated by Unattended Ground Sensor (UGS) sensors when several targets evolve in close formation. Our future research works will consist to: 1) use other cost functions for the TSA algorithm by introducing the entropic distance and evaluate the performances obtained, 2) detect the conflicts between the segment association and let the

Algorithm \ Target		1	2	3	4	5	6	7	8	9	10
TSA wo class info.	TSP	0.56	0.77	0.68	0.67	0.92	0.67	0.76	0.74	0.76	0.64
	PCC	0	0	0	0	0	0	0	0	0	0
TSA w class info. scoring	TSP	0.70	0.80	0.88	0.61	0.90	0.69	0.87	0.79	0.81	0.94
	PCC	0.41	0.61	0.44	0.47	0.29	0.37	0.08	0.43	0.59	0.03
TSA w class info. gating	TSP	0.74	0.89	0.83	0.84	0.93	0.80	0.86	0.80	0.88	0.94
	PCC	0.45	0.62	0.35	0.61	0.31	0.58	0.11	0.55	0.77	0.03
Algorithm \ Target		11	12	13	14	15	16	17	18	19	20
TSA wo class info.	TSP	0.50	0.85	0.59	0 69	0.58	0.79	0.58	0.76	0.65	0.53
	PCC	0	0	0	0	0	0	0	0	0	0
TSA w class info. scoring	TSP	0.90	0.88	0.79	0.81	0.76	0.72	0.68	0.80	0.52	0.43
	PCC	0.44	0.40	0.21	0.67	0.70	0.41	0.21	0.22	0.02	0.29
TSA w class info. gating	TSP	0.93	0.87	0.86	0.82	0.96	0.83	0.68	0.69	0.77	0.86
	PCC	0.62	0.42	0.40	0.61	0.66	0.55	0.22	0.20	0.03	0.59

Table II: MOP of the TSA algorithm without class information.

operator to take a decision, 3) use the conflict detector and the UGS location to automatically differ the TSA algorithm execution, 4) study the problem of UGS deployment by taking into account the contextual information, and 5) work on the signal processing to improve the GMTI classification information.

REFERENCES

[1] B. Pannetier, K. Benameur, V. Nimier, and M. Rombaut, "VS IMM using road map information for ground target tracking," *Proceedings of International Conference on Information Fusion 2005, Philadelphia, USA*, Jul. 2005.

[2] S. Blackman and R. Popoli, *Design and analysis of modern tracking systems*. 1999.

[3] E.Blasch and L. Hong, "Simultaneous feature-based identifications and track fusion," *Proceedings of the IEEE Conference on decision and Control, Tampa, FL*, Dec. 1998.

[4] E.Blasch and T. Connare, "Feature aided JBPDAF group tracking and classification using a IFFN sensor," *Proceedings of SPIE*, Dec. 2002.

[5] E.Blasch and B. Kahler, "Multi-resolution EO/IR tracking and identification," *Proceedings of International Conference on Information Fusion 2005, Philadelphia, USA*, Jul. 2005.

[6] T. K. Y. Bar-Shalom and C. Gokberk, "Tracking with classification-aided multiframe data association," *IEEE Transactions on aerospace and electronic systems*, 2005.

[7] B. Pannetier, J. Dezert, and P. Maupin, "Multiple ground target tracking and classification with DSmT," *Proceedings of GI Jahrestagung, Leipzig*, Oct. 2010.

[8] S. Zhang and Y. Bar-Shalom, "Track segment association for GMTI tracks of evasive move-stop-mve maneuvering targets," *Proceedings of IEEE aerospace and electronics systems*, Jul. 2011.

[9] Y. Bar-Shalom and D. Blair, *Multitarget multisensor tracking : Applications and Advances*. Artech House, 2000.

[10] B. Pannetier, J. Dezert, and E. Pollard, "Improvement of multiple ground targets tracking with GMTI sensors and fusion identification attributes," *Proceedings of IEEE Aerospace Conference*, Mar. 2008.

[11] B. Pannetier, V. Nimier, and M. Rombaut, "Multiple ground target tracking with a GMTI sensor," *Proceedings of Multi-sensor Fusion Information conference*, Sept 2006.

[12] NATO, *STANAG 4607 JAS (Edition 2) - NATO ground moving target indicator GMTI format*. 2007.

[13] D. Bizup and D. Brown, "The over extended Kalman filter − Don't use it!," *Proceedings of International Conference on Information Fusion 2003, Cairns, Australia*, Jul. 2003.

[14] D. I. S. Agency, "Common Warfighting Symbology, MIL-STD 2525C," tech. rep., Technical document, IPSC, 2008.

[15] Y. Bar-Shalom and X. R. Li, *Multitarget-multisensor tracking: Principles and techniques*. YBS oublisher, 1995.

[16] T. Kirubarajan and Y. Bar-Shalom, "Tracking evasive move-stop-move targets with an MTI radar using a VS-IMM estimator," *proceedings of IEEE Transactions on aerospace and electronic systems*, 2003.

[17] B. J. Noe and P. E. N. Collins, "Variable structure interacting multiple model filter VS-IMM for tracking targets with transportation network constraints," *Proc. of SPIE, Signal and Data Processing of Small Targets*, 2000.

[18] P. Shea, T. Zadra, D. K. E. Frangione, and R. Brouillard, "Improved state estimation trough use of roads in ground tracking," *Proceedings of SPIE, Signal and Data Processing of Small Targets*, 2000.

[19] X. R. Li and Y. Bar-Shalom, *Multitarget/Multisensor Tracking Applications and Advances Volume III, Chapter X*. Artech House, 2000.

[20] A. Wald, "Sequential tests of statistical hypotheses," *Annals of Mathematical Statistics*, Jun. 1945.

[21] S.-W. Yeom, T. Kirubarajan, and Y. Bar-Shalom, "Improving track continuity using track segment association," *Proceedings of IEEE Aerospace Conference*, Mar. 2003.

[22] M. Sundkvist and N. Bergman, "Fixed lag smoothing for target tracking applications based on IMM," *Proceedings of IEE worshop target tracking: algorithms and applications*, 2001.

[23] N. Nandakumaran, T. Lang, M. McDonald, and T. Kirubarajan, "Interacting multiple model forward filtering and backward smoothing for maneuvering target," *Proceedings of IEEE aerospace and electronics systems*, 2012.